

## Self-similarity and structure of DLA and viscous fingering clusters

This article has been downloaded from IOPscience. Please scroll down to see the full text article.

1989 J. Phys. A: Math. Gen. 22 L271

(<http://iopscience.iop.org/0305-4470/22/7/004>)

View [the table of contents for this issue](#), or go to the [journal homepage](#) for more

Download details:

IP Address: 129.252.86.83

The article was downloaded on 01/06/2010 at 07:58

Please note that [terms and conditions apply](#).

## LETTER TO THE EDITOR

# Self-similarity and structure of DLA and viscous fingering clusters

Einar L Hinrichsen, Knut Jørgen Måløy, Jens Feder and Torstein Jøssang  
Department of Physics, University of Oslo, Box 1048, Blindern, 0316 Oslo 3, Norway

Received 8 February 1989

**Abstract.** Diffusion-limited aggregation clusters and the structures observed in viscous fingering experiments at high capillary numbers are tree-like fractals. The different branches may be assigned a *branch order* in a way that exhibits scaling, and permits a self-similar characterisation in terms of the bifurcation ratio  $r_N$  and the length ratio  $r_L$  of branches of different orders. The fractal dimension is given by  $D = \ln(r_N)/\ln(1/r_L)$ . Good agreement between experiments and simulations is found. A crossover function characterises the branch orders.

The diffusion-limited aggregation model [1] (DLA) generates fractal [2] structures and is the prototype of 'Laplacian' [3, 4] growth models that lead to ramified tree-like structures. In simulations of the DLA model one finds that the radius of gyration  $R_g$  of the growing cluster scales with the mass  $M$  of the cluster as [5]  $M \sim R_g^D$  where  $D_g$ , the radius-of-gyration dimension or growth dimension, is 1.71 in two, and 2.5 in three dimensions. Many two-dimensional growth processes exhibit regimes where the observed structures resemble DLA clusters with  $D \approx 1.7$  [6]. The analogy between DLA and viscous fingering (VF) in porous media was first pointed out by Paterson [7] and a modified DLA model [8] simulates the observed VF dynamics accurately. For a discussion of irreversible growth models see [6] and [9].

DLA clusters have different scaling properties in the radial and azimuthal directions [10]. This gives rise to the questions: is DLA self-similar? In spite of the recent progress of a renormalisation group approach [14] in estimating the fractal dimension of DLA, much remains to be done, particularly in reconciling the many *different* fractal dimensions that arise when DLA-like structures are analysed; see table 1.

We introduce a *new* way to characterise DLA clusters and VF patterns in terms of a hierarchy of *branch orders*. The concept of branch orders has previously been used by Horton [11]† in the description of river systems. However, to our knowledge this is the first time this concept has been used for physical systems. Horton found that the bifurcation ratio  $r_N$  between the number of streams of two subsequent orders was constant for many river systems. He also found that the length ratio  $r_L$  between two subsequent orders was constant. For DLA and other branching structures without loops it is possible to assign branch orders in the following way. Each branch defines a continuous line, starting at a tip, and ending on another branch of lower order if it is not the 'trunk' (zeroth-order branch). More than two branches may meet at a single

† For a discussion see [9, § 12.2], but note that there is an erroneous expression for  $D$  in the first and second printing.

Table 1. Fractal dimensions for DLA and VF.

		DLA	VF
Branch order ratios			
$r_N = N_n/N_{n-1}$	Number	$5.2 \pm 0.2$	$4.8 \pm 0.5$
$r_L = L_n/L_{n-1}$	Length	$0.35 \pm 0.01$	$0.34 \pm 0.04$
Dimensions			
$D_s = \frac{\ln(r_N)}{\ln(1/r_L)}$	Self-similarity	$1.6 \pm 0.1$	$1.5 \pm 0.1$
$N(\delta) \sim \delta^{-D_b}$	Box	$1.62 \pm 0.02^\dagger$	$1.51 \pm 0.06$
$N(\delta) \sim \delta^{-D_b}$	Box $^\ddagger$	$1.67 \pm 0.03$	—
$M(R_g) \sim R_g^{D_g}$	Growth	$1.710 \pm 0.005$	—
$M(r) \sim r^{D_c}$	Cluster	$1.69 \pm 0.01^\dagger$	$1.62 \pm 0.05^\dagger$

$^\dagger$  Estimated by scaling different cluster sizes onto the same curve.

$^\ddagger$  Box-counting only points with  $r < R_g$ .

point. The highest-order branches are those which have no side branches. The next-to-highest-order branches have side branches of the highest order, and so on. If branches of the same order  $n$  meet, the longest branch is relabelled and assigned order  $n - 1$ . The minimal side branch order of a given point on a branch is the lowest side branch order found when going from the tip to this point. A unique assignment of branch orders is obtained if the minimal side branch order does not decrease in steps larger than one when going from the tip to the root point.

We have discovered that both DLA clusters and VF patterns have a branching ratio  $r_N$  and a length ratio  $r_L$  independent of branch order  $n$ . The self-similarity of these statistical tree-like structures is therefore analogous to well known deterministic recursive structures such as the triadic Koch curve [2]. We also find for DLA and VF that the longest ( $n = 0$ ) branches are one dimensional. The higher-order branches are (for a given  $n$ ) fractally distributed on scales above their average length  $L_n$  and one dimensional on scales below  $L_n$ . This behaviour is characterised by a *crossover function* intrinsic to DLA and VF. Numerically we find good agreement between simulations and experiments, lending further support to the hypothesis that VF and DLA are in the same universality class.

The hierarchical ordering of self-similar fractal trees is best illustrated by discussing a deterministic algorithm as defined in figure 1. The *initiator* [2] shown in (a) is a line segment. The *generator* (b) replaces this line segment by  $\mathcal{N} = 5$  new line segments each scaled down by the ratio  $r = \frac{1}{3}$ . In (c) the generator is applied again giving the second-generation *prefractal* [9]. After an infinite number of applications of this algorithm one arrives at a fractal set. This set is self-similar and has a similarity dimension [2, 9]  $D_s = \log(\mathcal{N})/\log(1/r) = 1.46 \dots$  equal to the fractal dimension of the set. Each piece of the fractal is a scaled-down version of the whole set, as is required for self-similar fractals.

The branches of this structure may be characterised as follows. In (a) we have a tree-like structure containing only the trunk, which we identify as a branch of order 0 and length 1. In (b) we have added two side branches of order 1 and length  $\frac{1}{3}$ . In (c) the structure contains one branch of order 0, 2 branches of order 1, and 10 new

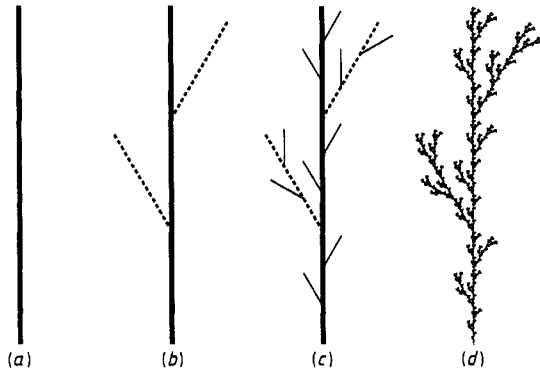


**Figure 1.** A recursively defined tree structure: —, a zeroth order branch; ---, first-order branches; —, second-order branches. The last figure is the result after seven iterations; see text for a full explanation.

branches of order 2. These new branches have a length of  $\frac{1}{5}$ . If we continue this process, we will at each stage have a branching prefractal with branches of order 0, 1, . . . . The number  $N_n$  and length  $L_n$  of branches of order  $n$  are given by

$$L_n = L_m r_L^{n-m} \quad \text{and} \quad N_n = N_m r_N^{n-m} \quad (1)$$

where in this example  $r_L = \frac{1}{5}$ ,  $r_N = 5$ , and  $m = 1$  is a lower cut-off for the validity of the scaling relations. In general the similarity dimension is given by  $D_s = \ln(r_N)/\ln(1/r_L)$  for three structures with fixed  $r_N$  and  $r_L$ .

This result is also obtained by a ‘box-counting’ procedure. Let the structure be covered by small ‘boxes’ having shapes chosen for optimal coverage but with the same length  $\delta = L_n$  and width  $\sim 2L_{n-1} \approx 2r_L\delta$ . Using (1) we find that the number of boxes needed to cover the fractal is given by

$$N(\delta) = \sum_{i=0}^n N_i L_i / \delta = A \left( \frac{\delta}{L_m} \right)^{-D} + B \left( \frac{\delta}{L_m} \right)^{-1} \quad (2)$$

where  $D = \ln(r_N)/\ln(1/r_L)$  is the fractal dimension.  $A$  and  $B$  are constants. The branches of order  $n = 0$  to  $n = m - 1$ , that do not follow the scaling relation in (1), contribute only to the last term in (2). This method of finding the fractal dimension using optimally shaped pieces to cover the fractal is closer to the Hausdorff-Besicovitch definition than the box-counting method [2]. Neglecting the corrections to scaling, i.e. the last term, in (2), we find that the number of pieces  $N(\delta)$  of ‘diameter’  $\delta$  needed to cover the fractal is given by

$$N(\delta) \sim \left( \frac{\delta}{L_m} \right)^{-D} \quad \text{with} \quad D = D_s = \frac{\ln(r_N)}{\ln(1/r_L)}. \quad (3)$$

This result shows that the fractal dimension for scaling trees is given by the similarity dimension. If one instead covers the fractal with square boxes of side  $\delta$ , one finds that the number of boxes needed to cover the fractal is  $N(\delta) \sim \delta^{-D_b}$ , where  $D_b$  is the box dimension [2].

We have analysed viscous fingering patterns obtained from experiments in a two-dimensional porous medium [8] and also computer-simulated off-lattice DLA clusters using these ideas. These structures have almost no loops, and may therefore be described as trees.

We generated 200 DLA clusters of size  $10^3$ , 50 of size  $5 \times 10^3$ , 30 of size  $2.5 \times 10^4$ , 20 of size  $5 \times 10^4$ , and 10 of size  $2.5 \times 10^5$ . Each particle added to the cluster was assigned a pointer to the particle to which it was attached. The tree structure was identified after the DLA seed particle in the centre was removed. To identify one branch, we started at the last particle and used the pointer to find the particle to which it was attached, and then to the particle to which this one was attached, and so on all the way to the DLA seed particle. The other branches were found in a similar way, keeping track of the branch order of the different branches. The fractal dimensions obtained for these clusters are summarised in table 1. There has been some discussion as to whether or not  $D_b$  is equal to  $D_g$ .<sup>12</sup> The crossover regime clearly visible for  $r > R_g$  in the cumulative mass within radius  $r$ ;  $M(r) = M(r/R_g)^{D_c} f(r/R_g)$  [8], may account for these discrepancies. Here  $M$  is the total mass or, equivalently, the total number of particles of a given cluster, and  $f$  is a crossover function.  $D_c$  is called the cluster dimension. Naively box-counting the whole cluster at a given stage of growth gives values of  $D_b$  in the range 1.59–1.63, depending on the range of  $\delta$  used in the fit. If the box-counting is limited to the part of the cluster inside a box of size  $R_g$ , we find values of  $D_b$  in the range 1.63–1.69. Even though this leads to an estimate of  $D_b$  lower than  $D_g$ , they may be equal within errors. Measuring  $D_c$  of the cumulative mass  $M(r)$  for  $r < R_g$  where  $f$  is constant, gives  $D_c = 1.69$ . The behaviour of the total mass  $M$  with respect to  $R_g$  necessarily includes the crossover regime. But if the mass and size of this regime still scales the same way,  $D_g$  should not be affected. Numerically the scaling  $M \sim R_g^{D_g}$  appears to be the most robust of the scaling relations we have tested, showing no sign of correction terms after a rather small initial growth. Instead we find that the local slope of  $\ln(M)$  as a function of  $\ln(R_g)$  has a small oscillatory behaviour around its mean value.

The experiments were carried out in a two-dimensional porous model 40 cm in diameter, consisting of a single random layer of 1 mm diameter glass beads glued between two glass plates. The experimental arrangement has been described before [8]. The pore space was initially filled with glycerol. Air at a constant pressure was then injected in the centre. The structures observed at high capillary numbers were the typical DLA-like viscous fingering structures [8]. The fractal dimensions given in table 1 were obtained by digitising photographs of the VF structures at a resolution of  $2000 \times 2000$  pixels. The branch orders were, however, identified manually from the pictures.

The branching ratio  $r_N$  and length ratio  $r_L$  were obtained by fitting the number and length of branches of order  $n$  to the power laws  $N_n \sim r_N^n$  and  $L_n \sim r_L^n$ . In the simulations, the average length of a branch was defined as either the average mass of the branch or the average tip-to-root distance of a branch. Both of these definitions gave approximately the same value for  $r_L$ . In the experiments, the average length of a branch was identified as the average mass. In figures 2 and 3 we show the experimental result together with results obtained from simulations for all the different cluster sizes. The points shown are the average values for these different cluster sizes. For a given size, the values fall on a straight line either above or below the average curve. The size of the cluster is, however, not correlated with this deviation from the average value. This scatter is instead related to the fact that averaging is done with fixed mass and not for a fixed maximal order. Note also that the scaling of the different cluster sizes in figure 3, show that  $R_g \sim L_n$  for all orders  $n$ , also orders  $n < m$  ( $\approx 2$  for DLA) that do not follow (1). Using this result in (3) gives the identification  $D_g = D_s$  since the total mass  $M \sim N(\delta) \sim R_g^{D_g}$ . The values of  $r_L$  and  $r_N$  do not change if the

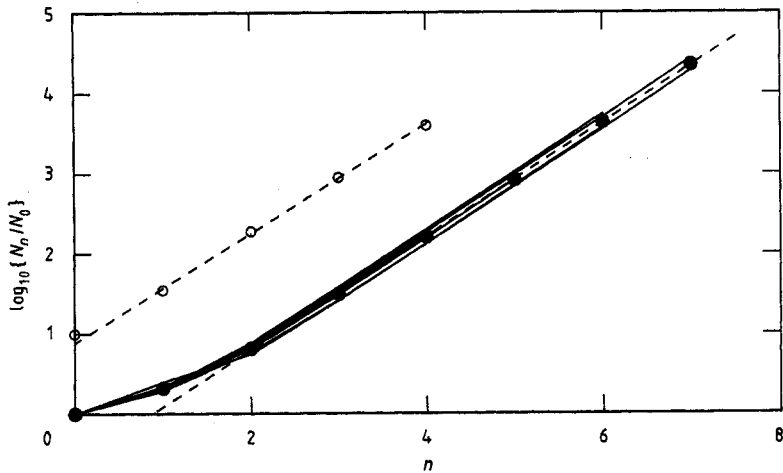


Figure 2. The number of branches  $N_n$  at a given order  $n$  for VF experiments (○) and DLA simulations (●). The lines represents fits of  $N_n \sim r_N^n$  to the data, with  $r_N = 4.8$  for VF and 5.2 for DLA. The experimental points have been shifted up one decade for clarity.

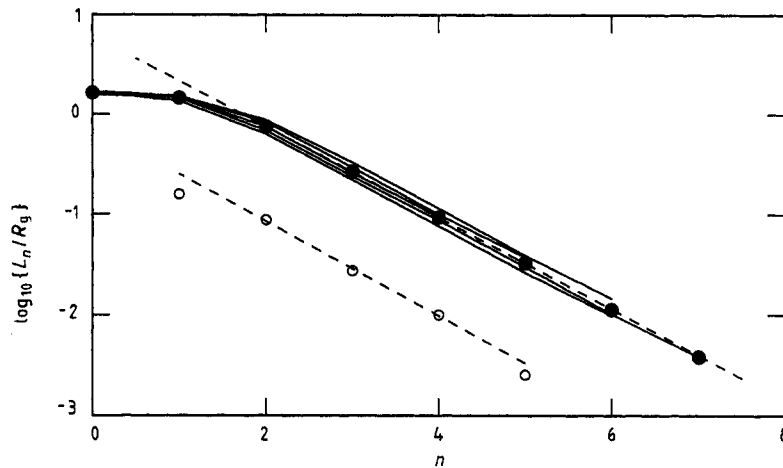
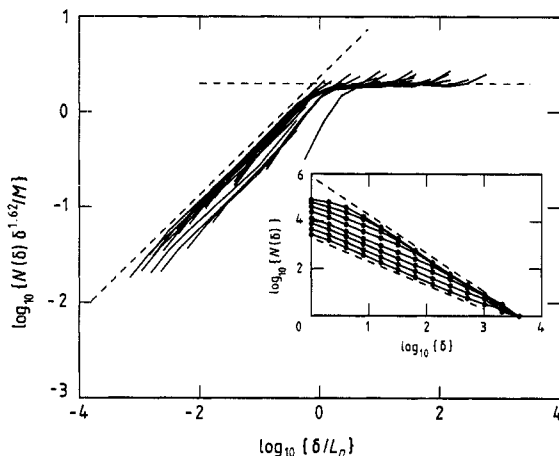


Figure 3. The scaled average length  $L_n/R_g$  plotted against branch order  $n$ .  $L_n$  is given by the tip-to-root distance in DLA (●) and the average mass in the VF experiments (○). Lines are fits of  $L_n \sim r_L^n$  to the data, with  $r_L = 0.34$  for VF and 0.36 for DLA. The experimental points have been shifted down for clarity.

analysis is limited to the part of the cluster within  $R_g$ . The scaling relations are therefore not changed in the crossover regime.

The two ratios characterising the branching structure of the tree-like fractals give  $D = 1.6$  from (3) for DLA clusters, consistent with other dimensions quoted in table 1. The viscous fingering result  $D = 1.5$  is also consistent with other values quoted in table 1.

For the DLA clusters, we have analysed each branch order separately in terms of the box counting algorithm. The insert in figure 4 shows the number  $N_n(\delta)$  of filled



**Figure 4.** The insert shows the result of box-counting individual orders for clusters of size  $2.5 \times 10^5$  particles. Slopes of broken lines are 1.0 (lower line) and 1.62 (upper line). The main figure shows the scaling function  $g(\delta/L_n)$  obtained by scaling similar curves for six different cluster sizes. Slope of broken line is 0.62.

boxes of order  $n$  as a function of the box size  $\delta$ . These curves have a linear regime,  $N_n(\delta) \sim \delta$ , for box sizes less than  $L_n$  and a fractal regime,  $N_n(\delta) \sim \delta^{-D}$ , for  $\delta$  larger than  $L_n$ . We therefore expect  $N_n(\delta)$  to have the scaling form

$$N_n(\delta) = M\delta^{-D}g(\delta/L_n). \quad (4)$$

The mass  $M$  is the total cluster mass. The crossover function  $g(x)$  is constant for  $\delta > L_n$  and tends to  $x^{D-1}$  for  $\delta < L_n$ . This is indeed demonstrated in figure 4, where all branch orders from clusters of six different sizes are scaled onto one single curve. Note that  $g(\delta/L_n)$  depend on  $n$  only through the ratio  $\delta/L_n$ . The length of the lowest orders is not fully grown because it is calculated by taking the mean value of different clusters of the same size and not at a given order. For that reason we cannot expect the lowest order to fit very well in the scaling plot, explaining some of the scatter seen. Also, as the insert in figure 4 shows, the higher-order branches cross over at small  $\delta$  to a slope close to 0 instead of 1. These branches consist of 1-2 particles and are therefore basically points. The highest-order branches from all the different cluster sizes collapse without scatter onto one curve in this regime, which is the curve that deviates most from the scaling function seen in figure 4.

We conclude that DLA and VF patterns are tree-like structures having fixed bifurcation and length ratios independent of branch order. From these two ratios, a fractal dimension may be defined analogous to the self-similarity dimension of deterministic self-similar fractals such as the deterministic tree in figure 1. This dimension is consistent with values obtained from other methods. We have shown that DLA and VF clusters are self-similar in terms of branch order. The branches of DLA are linear on length scales less than the average branch length, and fractally distributed on larger scales. This feature is characterised by the scaling function  $g(\delta/L_n)$ , valid for all but the largest and smallest branches. We have also shown that the lengths  $L_n$  all scale with  $R_g$ .

Comparing the results obtained both from the simulations of the DLA clusters, and the viscous fingering experiments at high capillary numbers, we see a close agreement

in both the bifurcation ratio and the length ratio. This lends further support to the hypothesis that these two processes are in the same universality class.

After the completion of this manuscript we received preprints [13] by J Vannimenus that analyse tree structures using 'Strahler numbers' which originally were used to analyse river systems [14]. Vannimenus investigates tree structures using this scheme, and he introduces a *ramification matrix*. The Strahler classification of branch orders is related to the Horton scheme, and we consider the two approaches to be complementary.

We thank A Aharony and P Meakin for very helpful and stimulating discussions. This work has been supported by VISTA, a research cooperation between the Norwegian Academy of Science and Letters and Den norske stats oljeselskap a.s. (STATOIL).

## References

- [1] Witten T A and Sander L M 1981 *Phys. Rev. Lett.* **47** 1400
- [2] Mandelbrot B B 1982 *The Fractal Geometry of Nature* (San Fransisco: Freeman)
- [3] Niemeyer L, Pietronero L and Wiesmann H J 1984 *Phys. Rev. Lett.* **52** 1033
- [4] Gould H, Family F and Stanley H E 1983 *Phys. Rev. Lett.* **50** 686  
Kolb M 1987 *J. Phys. A: Math. Gen.* **20** L285  
Nagatani T *J. Phys. A: Math. Gen.* **20** 6603  
Pietronero L, Erzan A and Evertsz C 1988 *Phys. Rev. Lett.* **61** 861
- [5] Meakin P 1983 *Phys. Rev. A* **27** 1495
- [6] Meakin P 1988 *Phase Transitions and Critical Phenomena* vol 12, ed C Domb and J L Lebowitz (New York: Academic) p 335
- [7] Paterson L 1984 *Phys. Rev. Lett.* **52** 1621
- [8] Måløy K J, Feder J and Jøssang T 1985 *Phys. Rev. Lett.* **55** 2688  
Måløy K J, Boger F, Feder J, Jøssang T and Meakin P 1987 *Phys. Rev. A* **36** 318
- [9] Feder J 1988 *Fractals* (New York: Plenum)
- [10] Meakin P and Vicsek T 1986 *Fractals in Physics* ed L Pietronero and E Tosatti (Amsterdam: North-Holland) pp 213-6
- [11] Horton R E 1945 *Bull. Geol. Soc. Am.* **56** 275
- [12] Argoul F, Arneodo A, Grasseau G and Swinney H L 1988 *Phys. Rev. Lett.* **61** 2558  
Meakin P 1988 *Proc. Erice Meeting on Fractals* ed L Pietronero (New York: Plenum) in press
- [13] Vannimenus J 1988 *Universalities in Condensed Matter* ed R Jullien, L Peliti, R Rammal and N Boccara (Berlin: Springer) in press  
Vannimenus J and Viennot X G 1989 *J. Stat. Phys.* in press.
- [14] Strahler A N 1952 *Bull. Geol. Soc. Am.* **63** 275